
# SLIDING RESISTANCE AT THE JOINT BETWEEN A STRUCTURAL WALL AND THE BASEMENT CEILING: A MECHANICAL MODEL

Harald SCHULER[1] and Burkhart TROST[2]

## ABSTRACT

The stabilization of tall buildings against earthquakes in many cases is realised by structural walls which are anchored in the basement box. When the anchorage length between the fixing points of the walls is small, a high shear force can occur. Additionally at the cold joint between the walls and the basement ceiling a weak point exists. Therefore an investigation on the sliding resistance at cold joints was launched at the FHNW.

This paper presents a mechanical model which is used to analyse the sliding resistance at the cold joint of nearly quadratic basement walls. The analysis is done on a building with a height of 40m and a basement wall size of 4m x 4m. In the parameter study the axial force and the reinforcement ratios, at the boundary and in the web, are varied. Analysed are the resistances of aggregate interlock, dowel action and the shear resistance of the reinforcement which is under compression. The study shows that for a quadratic wall in most cases, failure due to sliding occurs before the maximum flexural deformation is reached. Thus the flexural ductility, e.g. in pushover analysis, is overestimated when the anchorage lengths of the structural wall is short. Therefore it is recommended for squat walls to take a previous sliding failure into account in a performance-based earthquake analysis.

## INTRODUCTION

Reinforced concrete structures under earthquake loads can be highly stressed in the zones where the structural walls are anchored into the basement. The forces and moments have to be transferred from the walls into the basement floor and the basement ceiling. Figure 1 shows the section under consideration. The construction of the basement proceeds from the basement slab to the walls and then to the basement ceiling. This leads to cold joints between the structural walls and the ceiling plate. Across this joint, the wall forces are transferred via aggregate interlock, dowel action, and a diagonal stress field in the compression zone. Under reversed cyclic loading, the concrete joint suffers a decrease in shear strength because of crack opening. Within the first two half-cycles - first and second half-cycle in Figure 2 - a crack emerges along the complete joint. If the vertical load carried by the wall is relatively small, crack closing in the compression zone only takes place up to a certain level, which results in a residual crack opening, thus enabling sliding. To study this phenomenon, experiments on compact sliding specimens are carried out by Trost et al. (2014).

[1] Prof. Dr.-Ing., University of Applied Sciences and Arts Northwestern Switzerland, harald.schuler@fhnw.ch
[2] Dipl.-Ing., University of Applied Sciences and Arts Northwestern Switzerland, burkhart.trost@fhnw.ch

In this paper a mechanical model is presented which implements sliding as an additional failure criterion to a nonlinear load-displacement curve. With the model, single effects like aggregate interlock (simulated as friction), dowel action or the load capacity of the diagonal stress field can be separated and quantified. This enables an insight into the single effects along the cold joint. The model is set up on the beam theory and therefore limited to walls with an aspect ratio $h_b/l_w$ not smaller than approximately 0.8.

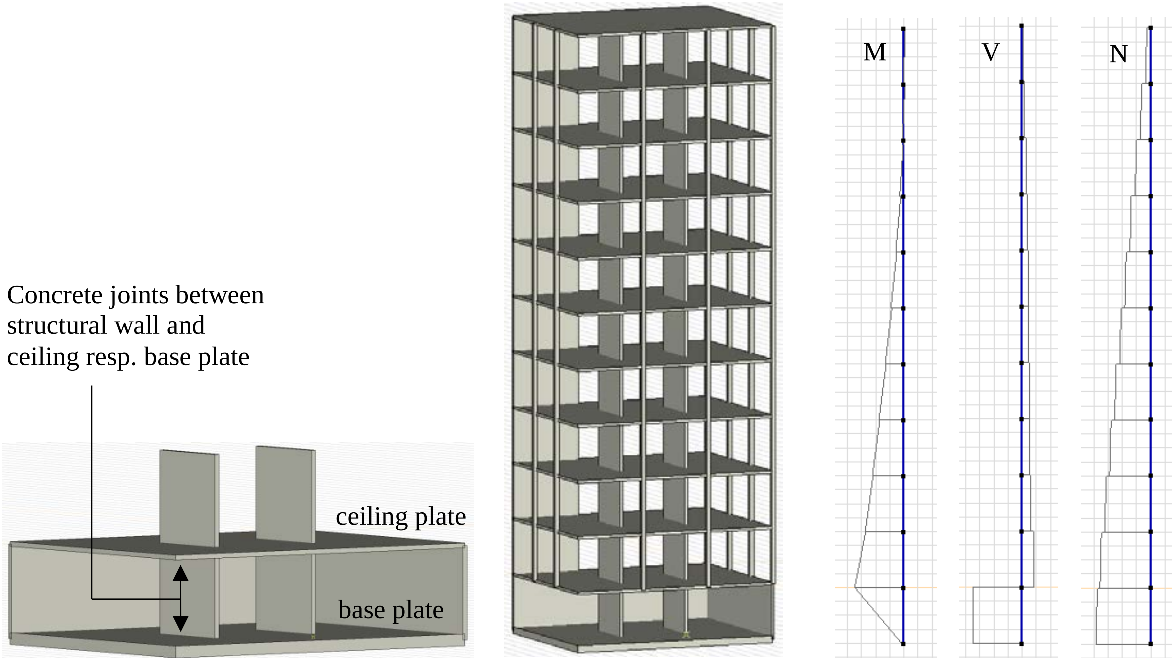


Figure 1. Concrete joints between the structural wall and the slabs (left); bending moment, shear - and axial force from the response spectrum analysis (right)

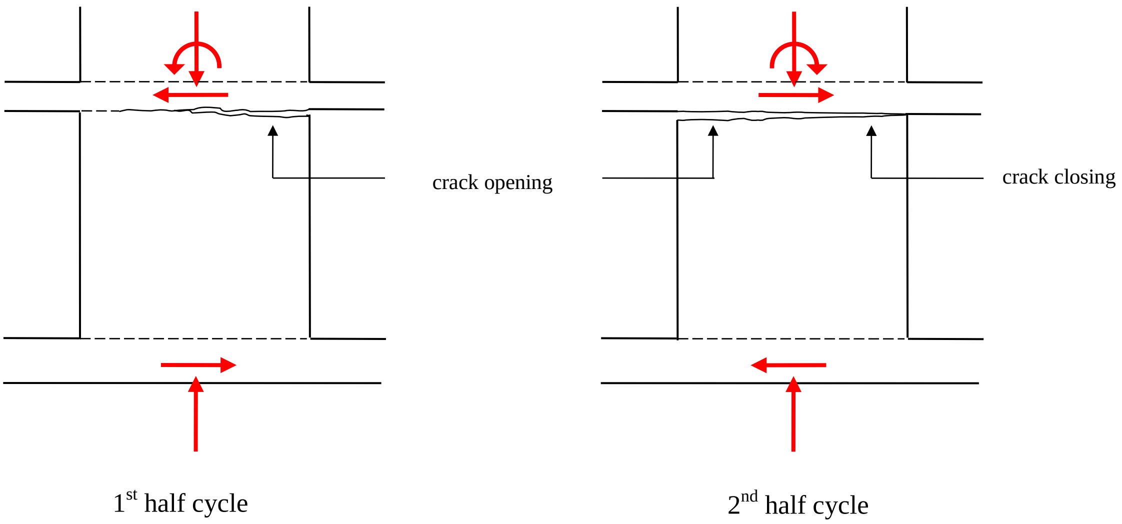


Figure 2. Crack opening process at the joint between the structural wall and the ceiling plate under reversed cyclic loading

## A SLIDING FAILURE CRITERION ALLOCATED TO THE BASEMENT SHEAR - TOP DISPLACEMENT CURVE

The concept of the model is to calculate the load-displacement curve and check the sliding resistance. To investigate the sliding resistance at the cold joint, the basement shear force $V_b$ is considered as the load and related to the top displacement $\delta_t$ of the building (cf. also Figure 5). The shear force at the anchorage $V_a$ can also be calculated from equation 3. For the investigated wall with $h_t$ = 40m and $h_b$ = 4m and a triangular load distribution $V_b/V_a$ is 6.7. The following three steps set up the model.

### 1. Moment-curvature curve (M-κ curve)

For the calculation of the momentum-curvature relationship, the cross-section type of Figure 4 is considered. Addressed are walls where the bending deformation dominates over the shear deformation which can be assumed when the ratio between the height and the length is higher than $h_b/l_w$ ~ 0.8. In the parameter study of this paper, a ratio of 1 is applied. To obtain the momentum-curvature relationship, the steel strain $\varepsilon_{s1}$ in the tension zone is predefined and the concrete boundary strain $\varepsilon_{c2}$ is solved under the condition that the sum of the vertical forces has to be equal to zero:

$$F_{s1} + F_{sw1,y} + F_{sw1,el} + F_{sw2} + F_{s2} + F_c + N = 0 \qquad \text{(positive in one direction)} \qquad (1)$$

- $F_c$: Flexural compression resultant of concrete
- $F_{s1}$: Flexural tensile resultant of the reinforcement $A_{s1}$
- $F_{s2}$: Flexural compression resultant of the reinforcement $A_{s2}$
- $F_{sw1,y}$: Flexural tensile resultant of the web reinforcement which yields: $a_{sw}\cdot x_{sw1,y}\cdot f_s$
- $F_{sw1,el}$: Flexural tensile resultant of the web reinforcement which is elastic: $a_{sw}\cdot x_{sw1,el}\cdot f_s/2$
- $F_{sw2}$: Flexural compression resultant of the web reinforcement: $a_{sw}\cdot x_{sw2,el}\cdot \varepsilon_{sw2}/2$ ($\varepsilon_{sw2}$ can be calculated geometrically from $\varepsilon_{c2}$ and remains elastic in all investigated cases.)

For the solution of the nonlinear equation, a numerical solver is used. The solved concrete strain $\varepsilon_{c2}$ also delivers the lengths x, $x_{sw1,el}$, $x_{sw1,y}$, $x_{sw2}$ and the forces $F_{s1}$, $F_{sw1,y}$, $F_{sw1,el}$, $F_{sw2}$, $F_{s2}$, $F_c$ which change for the predefined steel strains $\varepsilon_{s1}$. With the distances of the forces from the centre of the cross section the bending moment for the moment-curvature curve can be calculated:

$$M = F_c\cdot(l_w/2-a) + F_{s1}\cdot(l_w/2-d_1) + F_{s2}\cdot(l_w/2- d_2) + F_{sw1,y}\cdot z_{sw1,y} - F_{sw1,el}\cdot z_{sw1,el} + F_{sw2}\cdot z_{sw2} \qquad (2)$$

The constitutive equations of concrete and steel are based on the Swisscode SIA 262:2013 and the instruction sheet SIA 2018: C30/37: $f_c$ = 30N/mm$^2$, $\varepsilon_{cu}$ = 4‰; B500B: $f_s$ = 500N/mm$^2$, $\varepsilon_{su}$ = 50‰, $E_s$ = 205kN/mm$^2$, $\varepsilon_y$ = 2.44‰. In Figure 3 the stress-strain relationships are illustrated.

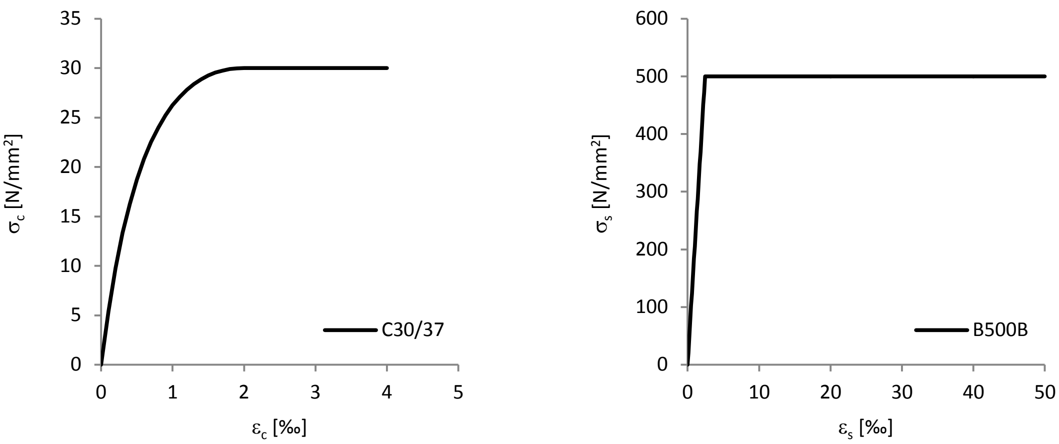


Figure 3. Constitutive equations of concrete and steel

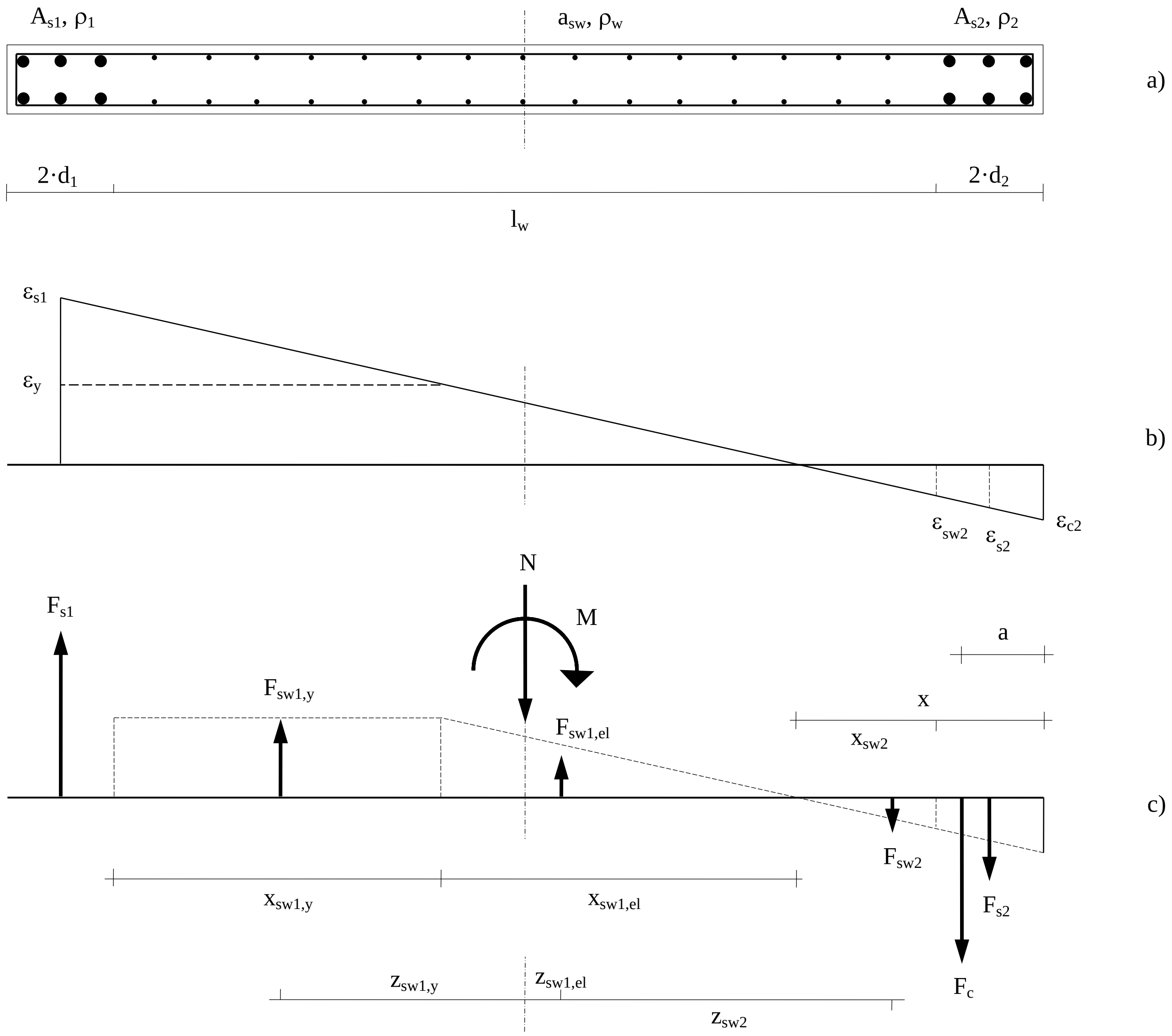


Figure 4. a) Cross section of a typical earthquake shear wall; b) strain distribution; c) forces

## 2. Basement shear – top displacement curve ($V_b$-$\delta_t$ curve)

The displacements at the top of the building $\delta_t$ are calculated for seven points of the moment-curvature curve. Figure 7 shows the points and the according steel strains $\varepsilon_{s1}$ = [0.5, 1.5, 2.44, 5, 10, 15, 25.8]‰ and concrete strains $\varepsilon_{c2}$ = -[0.38, 0.62, 0.86, 1.31, 2.05, 2.72, 4.0]‰. The calculation is done with the principle of virtual forces for the flexural displacement $\delta_{flex}$ and the rotation angle $\phi$ at the anchorage in the basement.

The first step is to calculate the load $q_t$ for the considered moment M of the moment-curvature curve. For a triangular load distribution, the second equation in (3) has to be solved for $q_t$. One obtains the load which corresponds to the clamping moment $M_a$. The next step is to calculate the line of the bending moment and the curvature along of $h_t$ and $h_b$. With these two lines, the flexural displacement and the rotation angle are calculated with the principle of virtual forces (equation (4)). Thus the relation of the top displacement $\delta_t = \phi \cdot h_t + \delta_{flex}$ to the shear force in the basement wall $V_b$ can be calculated. The necessary virtual load cases 1 for the rotation angle and the flexural displacement are illustrated in the 5th and 6th row of Figure 5. The displacement is used in the parameter study as the X-values in the Figures 7 to 11.

$$V_a = \frac{1}{2} \cdot q_t \cdot h_t; \qquad M_a = \frac{1}{3} \cdot q_t \cdot {h_t}^2; \qquad V_b = \frac{M_E}{h_b} = \frac{1}{3} \cdot q_t \cdot h_t \cdot \frac{h_t}{h_b} = \frac{2}{3} \cdot \frac{h_t}{h_b} \cdot V_a \tag{3}$$

$$\delta_{flex} = \int_0^{h_t} \kappa(x) \cdot M_1(x) dx; \qquad \phi = \int_0^{h_b} \kappa(x') \cdot M_1(x') dx'; \qquad \delta_t = \delta_{flex} + \phi \cdot h_t \tag{4}$$

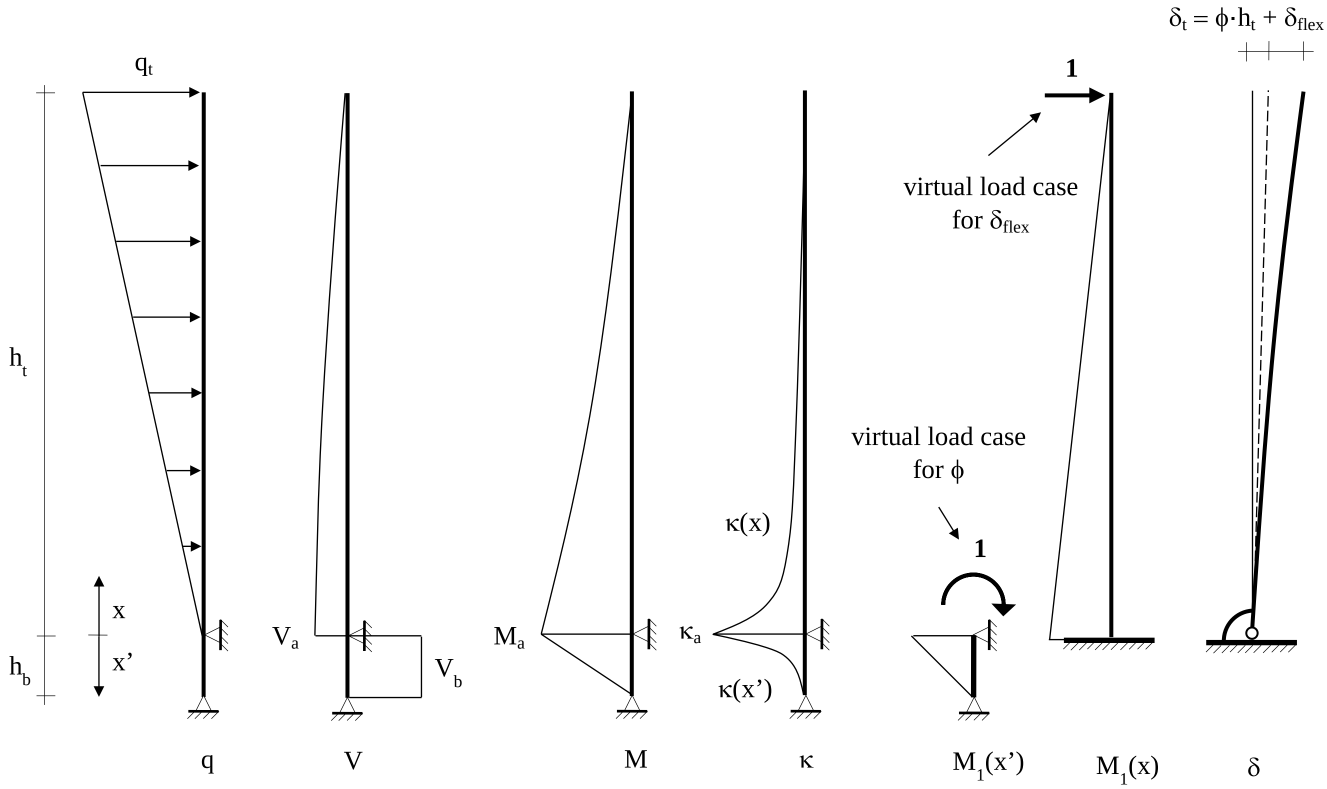


Figure 5. Calculation of the displacement $\delta_t$ at the top of the building with the principle of virtual forces

## 3. Sliding resistance

The sliding resistance comprises several effects, which are specified in equations 5 to 9 and listed below. With equation 10, the sum of the single effects is built. The calculation is done at seven points on the moment-curvature curve and provides thus an additional sliding failure criterion allocated to the basement shear force – top displacement curve ($V_b$-$\delta_t$ curve). In Figures 7 to 11, this failure criterion is added as $V_{slid}$ to the $V_b$-$\delta_t$ curve denoted as $F_{flex}$.

The single effects of sliding are:

- $V_c$: Friction resistance due to aggregate interlock of concrete in the compression zone, limited by the resistance of the inclined compression stress field resultant $C_{max}$
- $V_{s2}$: Shear resistance of the reinforcement $A_{s2}$ in the compression zone
- $V_{sw2}$: Shear resistance of the web reinforcement $x_{sw2} \cdot a_{sw}$ in the compression zone
- $V_{sw1}$: Resistance due to dowel action of the web reinforcement $x_{sw1,el} \cdot a_{sw}$ in the tension zone
- $V_{s1}$: Resistance due to dowel action of the reinforcement $A_{s1}$ in the tension zone, if $\varepsilon_{s1} < \varepsilon_y$

In the parts of the cross-section where the yield strain is exceeded, no sliding resistance of the steel can be activated. The steel is already utilized through bending. In parts where the steel is elastic, the residual stress up to the yield strength is available for sliding resistance. The interaction of bending und sliding is approximated with $[1-(\varepsilon_s/\varepsilon_y)^2]$, according to Zilch (2010).

The resistance of concrete $V_c$ due to aggregate interlock in the compression zone is described by a friction model ($\mu_c$=0.7) and is limited through the strength of the inclined compression stress field $V_{c\_max}$ (cf. centre right in Figure 7 to 11). For the strength, the concrete compression strength softening factor $k_c$ is set to 0.882, which is the mean value of the stress-strain relationship in Figure 3. Figure 6 b) illustrates the derivation of the sliding resistance of the inclined compression stress field. The angle $\alpha$ is obtained from the residual capacity of the stress field after bending (cf. equation 6 and bottom left in Fig. 7 to 11). The factor c in equation (9) for the description of dowel action is set to 1.3 (Zilch 2010). Cohesion is not applied because of complete crack opening within the first two half cycles.

$$V_c = \min[V_{c\_\mu};\ V_{c\_max}]; \qquad V_{c\_\mu} = \mu_c \cdot F_c \tag{5}$$

$$V_{c\_max} = k_c \cdot f_c \cdot x \cdot t_w \cdot \sin(\alpha) \cdot \cos(\alpha)\,; \qquad \alpha = \arcsin\left[\sqrt{\frac{F_c}{k_c \cdot f_c \cdot x \cdot t_w}}\right] \tag{6}$$

$$V_{s2} = A_{s2} \cdot f_s \cdot \left[1 - \left(\frac{\varepsilon_{s2}}{\varepsilon_y}\right)^2\right] \tag{7}$$

$$V_{sw2} = a_{sw} \cdot x_{sw2} \cdot f_s \cdot \left[1 - \left(\frac{0.5 \cdot \varepsilon_{sw2}}{\varepsilon_y}\right)^2\right] \tag{8}$$

$$V_{sw1} = a_{sw} \cdot x_{sw1,el} \cdot c \cdot (f_c \cdot f_s)^{0.5} \cdot \left[1 - \left(\frac{0.5 \cdot \varepsilon_y}{\varepsilon_y}\right)^2\right] = a_{sw} \cdot x_{sw1,el} \cdot c \cdot (f_c \cdot f_s)^{0.5} \cdot 0.75 \tag{9}$$

$$V_{slid} = V_c + V_{s2} + V_{sw2} + V_{sw1} \tag{10}$$

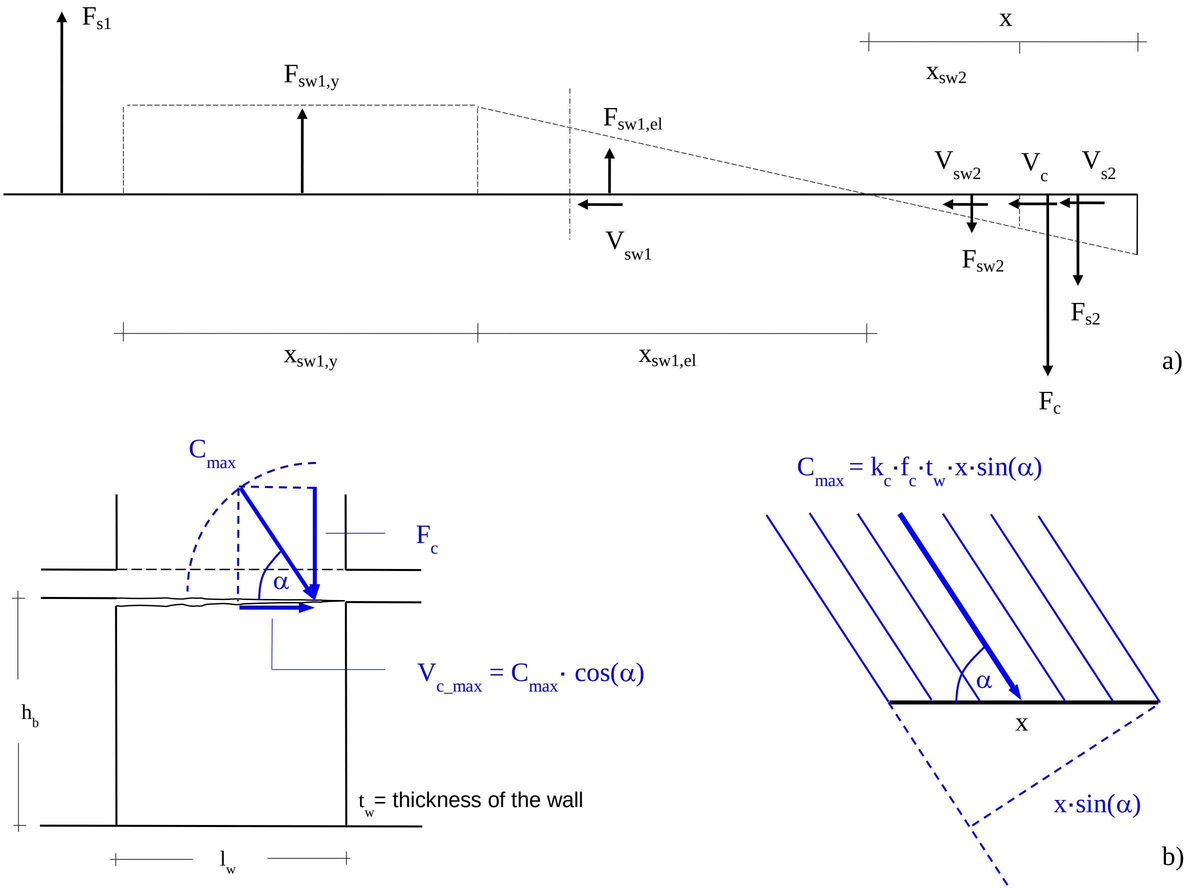


Figure 6. Components of the sliding resistance ($V_c$, $V_{s2}$, $V_{sw2}$, $V_{sw1}$) and maximum sliding resistance $V_{c\_max}$ due to the load capacity of the inclined stress field

## PARAMETER STUDY

The parameter study considers a building with a height of $h_t$ = 40m which is stabilized through two shear walls in each direction with the dimensions of $l_w$ = 4m and $t_w$ = 0.4m. The anchorage length in the basement is $h_b$ = 4m, which is a ratio of $h_t / h_b = 10$. The results of the study are shown in the Figures 7 to11 where the dots in the curves correspond to seven selected strain distributions which are listed in the lower right box. For the first two dots, $\varepsilon_{s1}$ is elastic; for the third it is $\varepsilon_{y;}$ and for the seventh, it is the failure point under flexure, which comes along with a failure of the compression resultant ($\varepsilon_{c2}$ = -4‰). $V_{slid}$ is the failure criterion due to sliding which is calculated at each dot of the $F_{flex}$-$\delta_t$ curve. In most cases, the $F_{flex}$-$\delta_t$ curve is intersected by the $V_{slid}$-$\delta_t$ curve, which leads to a reduction in the deformation capacity and hence of the ductility. The ductility is obtained from a bilinear idealisation of the $F_{flex}$-$\delta_t$ curve. Table 1 summarises the reduction of ductility for five different configurations.

M: Bending moment
$F_{flex}$: Basement shear force as a function of the displacement at the top of the building ($V_b$-$\delta_t$ curve)
$F_{push}$: Bilinear idealisation of the basement shear force – top displacement curve
$V_{slid}$: Sliding resistance at the cold joint (sum of the following single effects)
$V_c$: Sliding resistance in the concrete compression zone: min[$V_{c\_\mu}$, $V_{c\_max}$]
$V_{c\_\mu}$: Sliding resistance due to concrete friction (aggregate interlock)
$V_{c\_max}$: Sliding resistance due to the inclined compression stress field of concrete
$V_{s2}$: Sliding resistance due to the residual shear resistance capacity after bending of $A_{s2}$
$V_{sw2}$: Sliding resistance due to the residual shear resistance capacity after bending of $A_{sw2}$
$V_{s1}$: Sliding resistance due to the residual load capacity of dowel action after bending of $A_{s1}$, if $\varepsilon_{s1} < \varepsilon_y$
$V_{sw1}$: Sliding resistance due to the residual load capacity of dowel action after bending of $A_{sw1}$
$\kappa$: Curvature
$\kappa_a$: Curvature at the anchorage in the basement
$\delta_t$: Displacement at the top of the building
$x_c$: Compression zone of concrete
$\alpha$: Angle of inclined (diagonal) stress field when the strength $k_c \cdot f_c$ in the stress field is reached

Table 1. Displacements at the top of the building and ductility reduction due to sliding for five wall configurations

| $\rho_1 = \rho_2$ [‰] | $\rho_w$ [‰] | n [-] | $\delta_{max}$ [m] | $\delta_y$ [m] | $\delta_{slid}$ [m] | $\mu_{max}$ [-] | $\mu_{slid}$ [-] | red [%] |
|---|---|---|---|---|---|---|---|---|
| 2 | 0.1 | -0.1 | 0.518 | 0.268 | 0.400 | 1.93 | 1.49 | 23 |
| 2 | 0.1 | 0 | 0.534 | 0.365 | 0.534 | 1.46 | 1.46 | 0 |
| 2 | 0.1 | -0.3 | 0.419 | 0.292 | 0.358 | 1.43 | 1.23 | 14 |
| 3 | 0.1 | -0.1 | 0.55 | 0.301 | 0.418 | 1.83 | 1.39 | 24 |
| 2 | 0.5 | -0.1 | 0.617 | 0.349 | 0.501 | 1.77 | 1.44 | 19 |

$\rho_1 = A_{s1}/(2 \cdot d_1 \cdot t_w)$: Boundary element longitudinal reinforcement ratio in the tension zone
$\rho_2 = A_{s2}/(2 \cdot d_1 \cdot t_w)$: Boundary element longitudinal reinforcement ratio in the compression zone
$2 \cdot d_1 = 0.1 \cdot l_w$: Length of the boundary tension zone of $A_{s1}$
$2 \cdot d_2 = 0.1 \cdot l_w$: Length of the boundary compression zone of $A_{s2}$
$\rho_w = a_{sw}/t_w$: Reinforcement ratio in the web
$\delta_{max}$: Maximum displacement at the top of the building (flexural failure point)
$\delta_y$: Yield displacement at the top of the building for a bilinear approximation of the basement shear force – top displacement curve
$\delta_{slid}$: Maximum displacement at the top of the building due to sliding failure (intersection of the sliding curve with the flexural curve – top right in Figure 7 to 11)
$\mu$: Ductility in the bilinear approximation (top right in Figure 7 to 11)

$$n = \frac{N}{k_c \cdot f_c \cdot l_w \cdot t_w}$$ Normalized axial force, negative for compression

## CONCLUSIONS

This paper presents a mechanical model for the calculation of the sliding resistance which is associated to the load-displacement curve. The model quantifies the single effects of aggregate interlock, shear and dowel action for the purpose of illustration and discussion.

In a parameter study, a quadratic basement wall is analysed, varying the axial force and the reinforcement ratios at the boundary and in the web. The following phenomena have been observed:

- In most cases, the maximum flexural deformation is not reached because sliding failure occurs already at a smaller deformation.
- The reduction of the maximum deformation due to sliding amounts to between 15 and 24% for a normalized axial force between n = -0.1 and -0.3. This leads to a reduction of the ductility between 14 and 24%.
- For an axial force of zero, a previous sliding failure was not found for the quadratic wall.
- The main amount of sliding resistance arises in the compression zone. For each of the five investigated configurations the diagonal stress field fails at the intersection point of the sliding failure criterion with the load-displacement curve. Thus, friction failure at the intersection point is not decisive. In addition to the concrete resistance, the shear resistance of the steel in the compression boundary zone amounts a crucial part.
- The amount of the dowel action in the tension zone is relatively small, even for a web reinforcement ratio of 0.5%.

This calculation study of the sliding resistance at the cold joint is based on the descriptions of the EC2 and Zilch (2010) under static loadings. The aim was, to set up a model which separates the single effects without a detailed consideration into the insight of the effects. As mentioned in the introduction, cyclic loading changes the conditions through a permanent crack opening along the joint, which leads e.g. to a reduction of the friction coefficient or the resistance of dowel action in the tension zone. This phenomenon should be analysed in further investigations more in detail (cf. Trost et al. 2014). Furthermore the model is only applied to one basement wall geometry of 4m x 4m and a building height of 40m. A further study will be more general, which is planned in the ACI-Journal.

## REFERENCES


Burgueno R, Liu X and Hines EM (2014) “Web Crushing Capacity of High-Strength Concrete Structural Walls: Experimental Study”, *ACI Structural Journal*, V.111, No.2, March-April 2014, pp. 235-246

Hines EM and Seible F (2004) “Web Crushing of Hollow Rectangular Bridge Piers”, *ACI Structural Journal*, V.101, No.4, July-Aug. 2004, pp. 569-579

Beyer K, Dazio A, Priestley MJN (2011) “Shear deformations of slender reinforced concrete walls under seismic loading”, *ACI Structural Journal*, V. 108, No. 2, March-April 2011, pp. 167–177

Trost B, Schuler H and Stojadinovic B (2014) “Experimental investigation of sliding on compact sliding specimens under cyclic loads”, *Proceedings of the 15th European Conference on Earthquake Engineering*, Istanbul, Turkey, 24-29 August

Zilch K and Zehetmaier G (2010) “Bemessung im konstruktiven Betonbau”, *Springer-Verlag Berlin Heidelberg, pp 627*

DIN EN 1992-1-1: Eurocode 2: Bemessung und Konstruktion von Stahlbeton- und Spannbetontragwerken – Teil 1-1: Allgemeine Bemessungsregeln und Regeln für den Hochbau; Deutsche Fassung EN 1992-1-1: 2004 + AC:2010, Januar 2011

SIA 262:2013: Betonbau. Schweizer Ingenieur- und Architektenverein, Zürich 2013

SIA 2018: Instruction sheet. Überprüfung bestehender Gebäude bezüglich Erdbeben. Schweizer Ingenieur- und Architektenverein, Zürich 2004


## APPENDIX

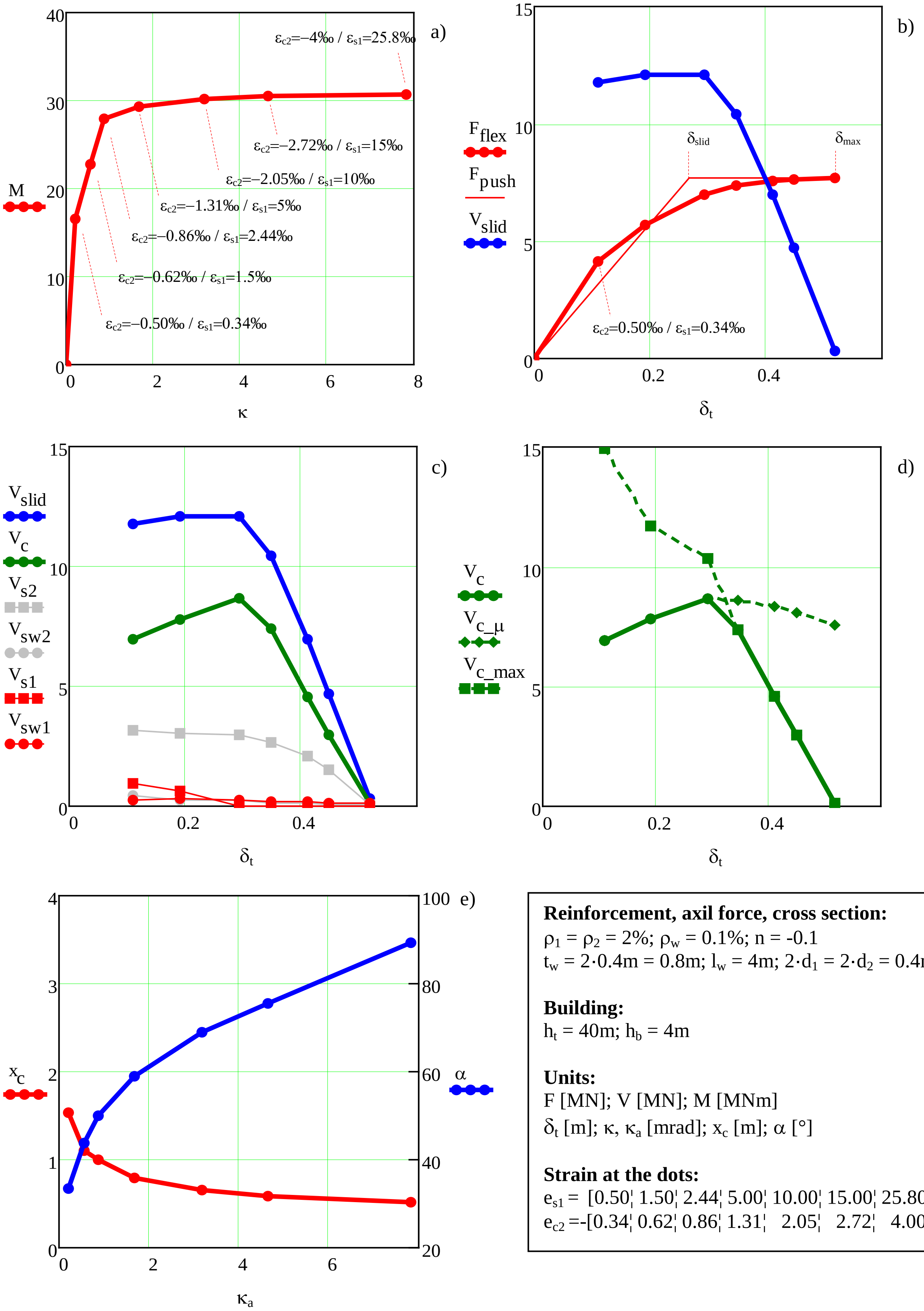


**Reinforcement, axil force, cross section:**
$\rho_1 = \rho_2 = 2\%$; $\rho_w = 0.1\%$; n = -0.1
$t_w = 2\cdot 0.4m = 0.8m$; $l_w = 4m$; $2\cdot d_1 = 2\cdot d_2 = 0.4m$

**Building:**
$h_t = 40m$; $h_b = 4m$

**Units:**
F [MN]; V [MN]; M [MNm]
$\delta_t$ [m]; κ, $\kappa_a$ [mrad]; $x_c$ [m]; α [°]

**Strain at the dots:**
$e_{s1}$ = [0.50¦ 1.50¦ 2.44¦ 5.00¦ 10.00¦ 15.00¦ 25.80]‰
$e_{c2}$ =-[0.34¦ 0.62¦ 0.86¦ 1.31¦ 2.05¦ 2.72¦ 4.00]‰

Figure 7. a) Moment - curvature curve; b) basement shear - top displacement curve ($F_{flex}$) + bilinear approximation ($F_{push}$) and sliding failure criterion ($V_{slid}$); c) sliding resistance due to concrete ($V_c$), dowel action ($V_{s1}$, $V_{sw1}$) and shear resistance ($V_{s2}$, $V_{sw2}$); d) sliding resistance of concrete friction ($V_{c\_\mu}$) and inclined compression stress field ($V_{c\_max}$); e) compression zone length ($x_c$) and angel of inclined compression stress field (α)

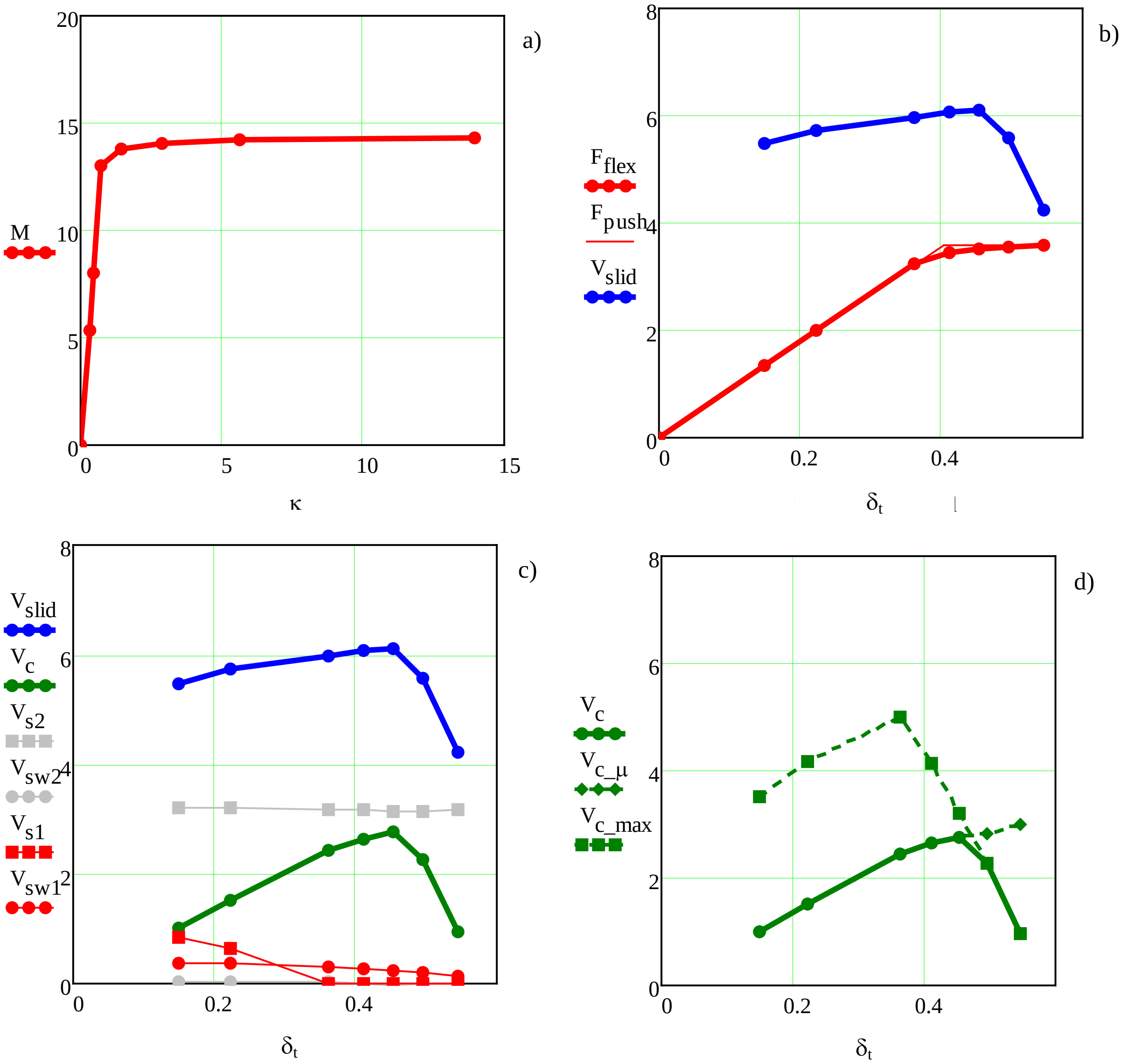


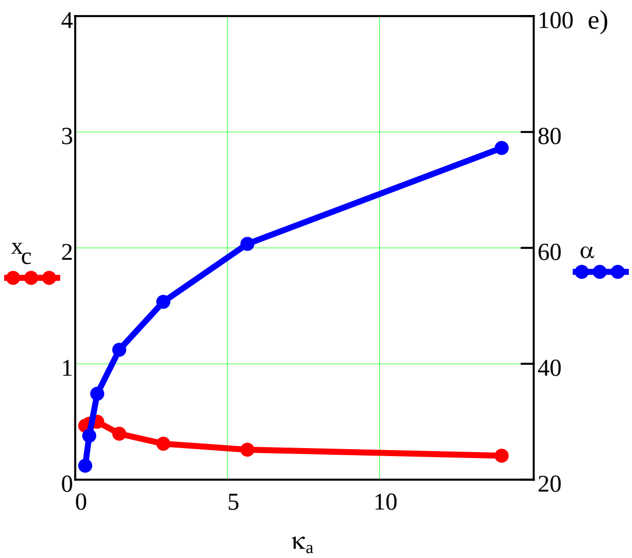


**Reinforcement, axil force, cross section:**
$\rho_1 = \rho_2 = 2\%$; $\rho_w = 0.1\%$; n = 0
$t_w = 2 \cdot 0.4m = 0.8m$; $l_w = 4m$; $2 \cdot d_1 = 2 \cdot d_2 = 0.4m$

**Building:**
$h_t = 40m$; $h_b = 4m$

**Units:**
F [MN]; V [MN]; M [MNm]
$\delta_t$ [m]; κ, $\kappa_a$ [mrad]; $x_c$ [m]; α [°]

**Strain at the dots:**
$\varepsilon_{s1}$ = [1.00¦ 1.50¦ 2.44¦ 5.00¦ 10.00¦ 20.00¦ 50.00]‰
$\varepsilon_{c2}$ = -[0.14¦ 0.22¦ 0.37¦ 0.58¦ 0.89¦ 1.42¦ 2.95]‰

Figure 8. a) Moment - curvature curve; b) basement shear - top displacement curve ($F_{flex}$) + bilinear approximation ($F_{push}$) and sliding failure criterion ($V_{slid}$); c) sliding resistance due to concrete ($V_c$), dowel action ($V_{s1}$, $V_{sw1}$) and shear resistance ($V_{s2}$, $V_{sw2}$); d) sliding resistance of concrete friction ($V_{c\_\mu}$) and inclined compression stress field ($V_{c\_max}$); e) compression zone length ($x_c$) and angel of inclined compression stress field (α)

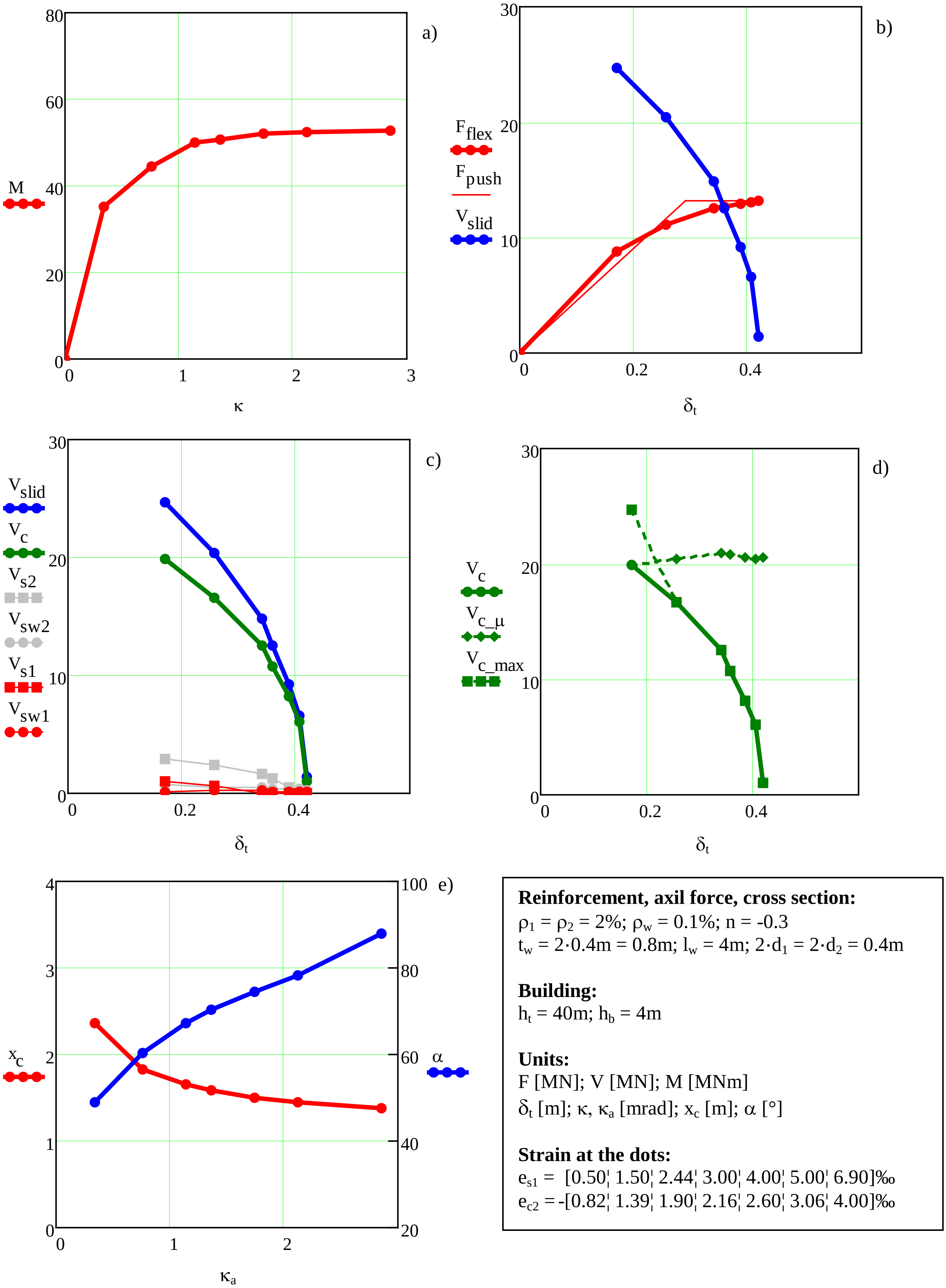


Figure 9. a) Moment - curvature curve; b) basement shear - top displacement curve ($F_{flex}$) + bilinear approximation ($F_{push}$) and sliding failure criterion ($V_{slid}$); c) sliding resistance due to concrete ($V_c$), dowel action ($V_{s1}$, $V_{sw1}$) and shear resistance ($V_{s2}$, $V_{sw2}$); d) sliding resistance of concrete friction ($V_{c\_\mu}$) and inclined compression stress field ($V_{c\_max}$); e) compression zone length ($x_c$) and angel of inclined compression stress field (α)

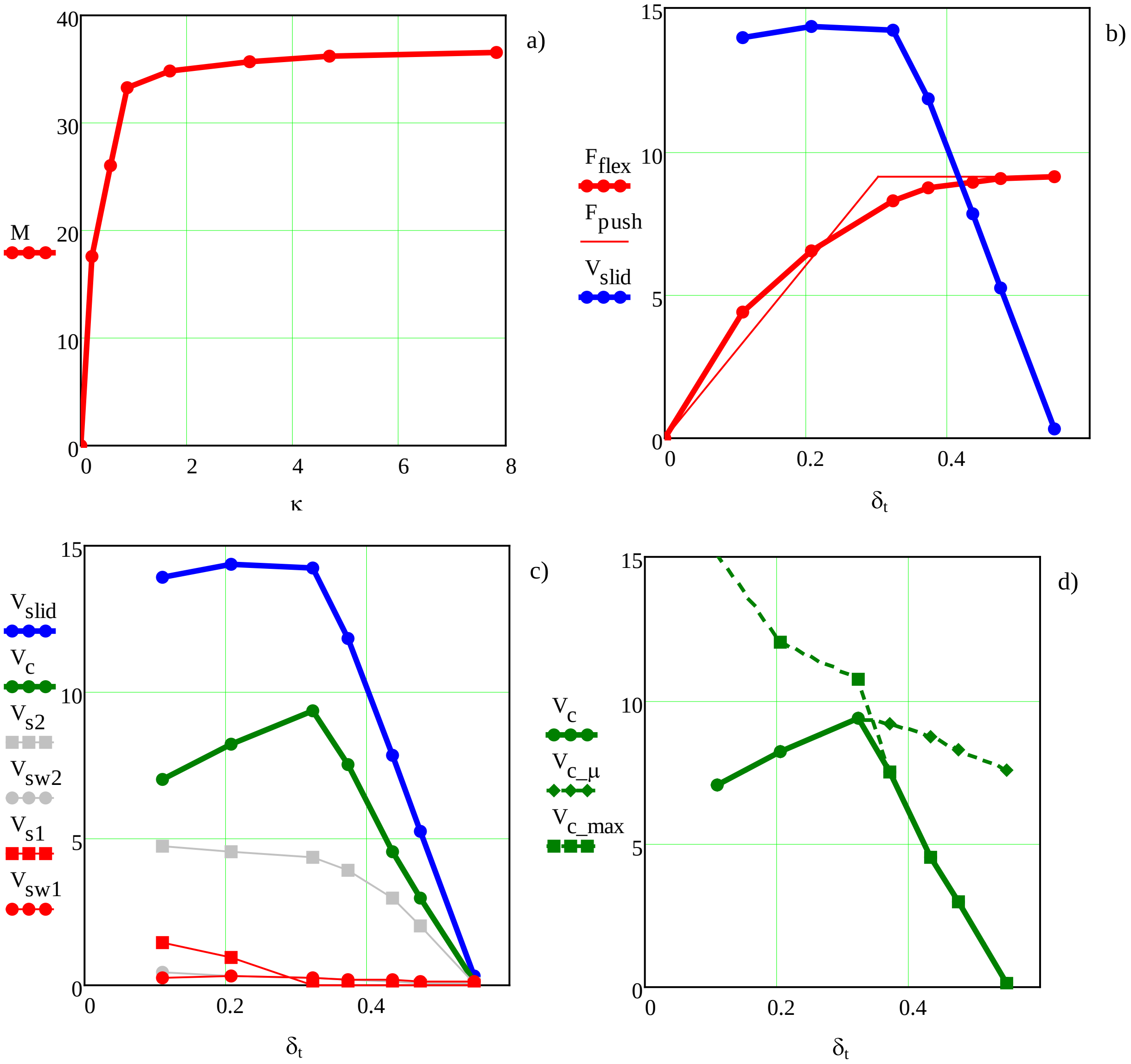


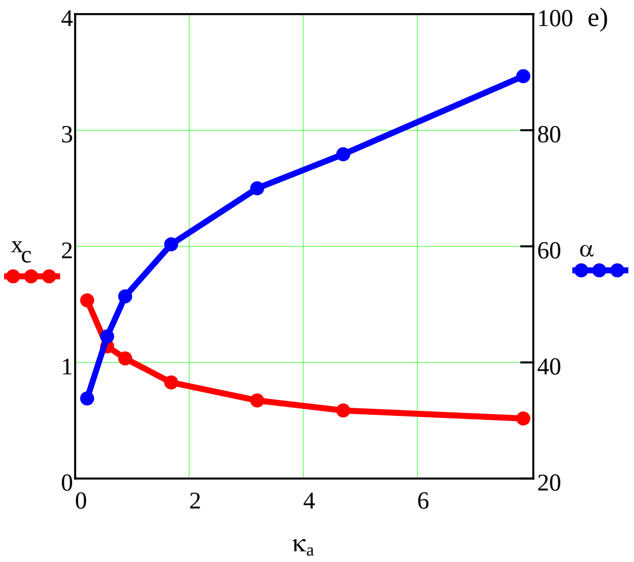


**Reinforcement, axil force, cross section:**
$\rho_1 = \rho_2 = 3\%$; $\rho_w = 0.1\%$; $n = -0.1$
$t_w = 2\cdot 0.4m = 0.8m$; $l_w = 4m$; $2\cdot d_1 = 2\cdot d_2 = 0.4m$

**Building:**
$h_t = 40m$; $h_b = 4m$

**Units:**
F [MN]; V [MN]; M [MNm]
$\delta_t$ [m]; $\kappa$, $\kappa_a$ [mrad]; $x_c$ [m]; $\alpha$ [°]

**Strain at the dots:**
$e_{s1}$ = [0.50¦ 1.50¦ 2.44¦ 5.00¦ 10.00¦ 15.00¦ 25.80]‰
$e_{c2}$ = -[0.34¦ 0.64¦ 0.92¦ 1.38¦ 2.13¦ 2.78¦ 4.00]‰

Figure 10. a) Moment - curvature curve; b) basement shear - top displacement curve ($F_{flex}$) + bilinear approximation ($F_{push}$) and sliding failure criterion ($V_{slid}$); c) sliding resistance due to concrete ($V_c$), dowel action ($V_{s1}$, $V_{sw1}$) and shear resistance ($V_{s2}$, $V_{sw2}$); d) sliding resistance of concrete friction ($V_{c\_\mu}$) and inclined compression stress field ($V_{c\_max}$); e) compression zone length ($x_c$) and angel of inclined compression stress field (α)

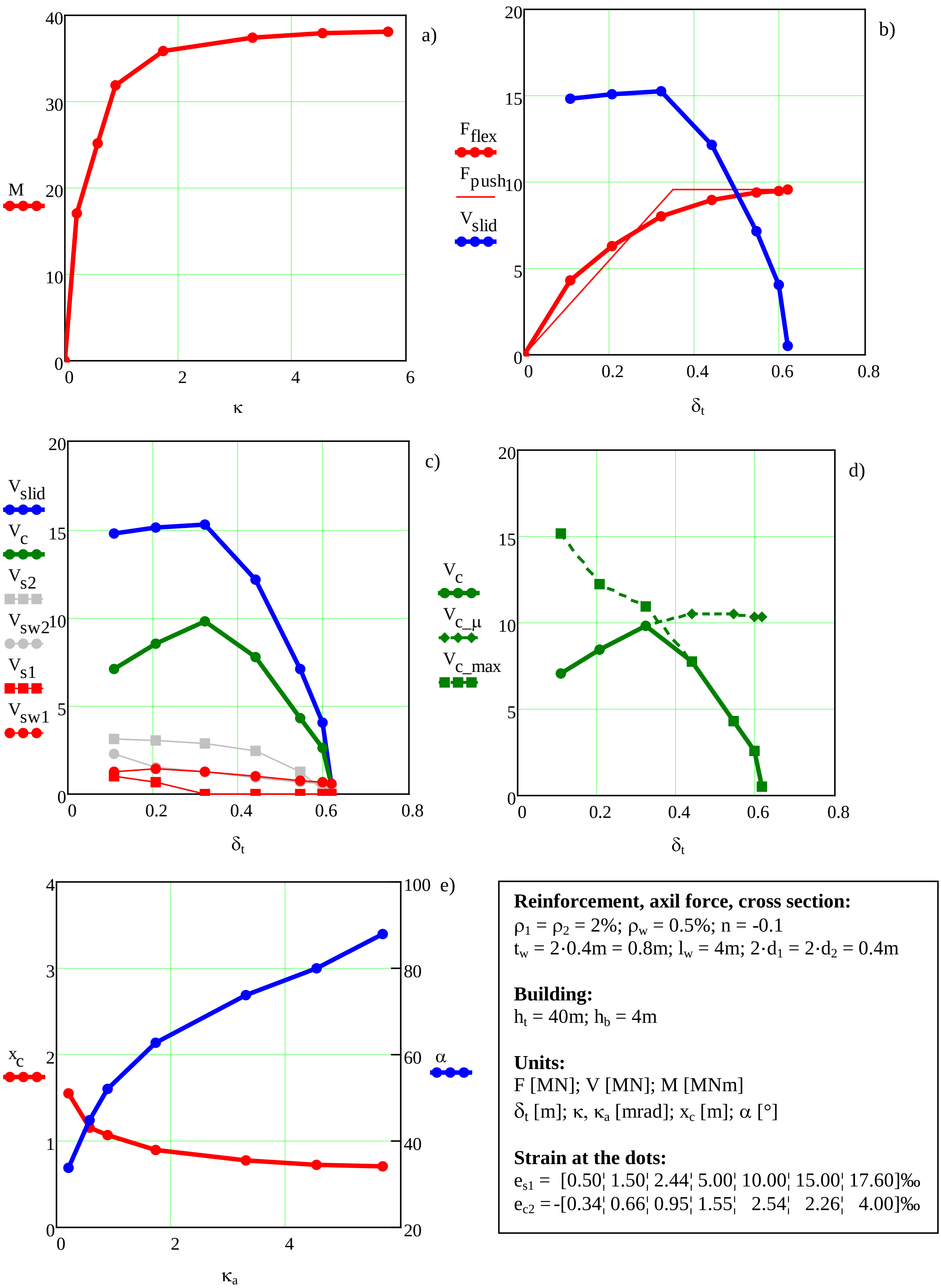


Figure 11. a) Moment - curvature curve; b) basement shear - top displacement curve ($F_{flex}$) + bilinear approximation ($F_{push}$) and sliding failure criterion ($V_{slid}$); c) sliding resistance due to concrete ($V_c$), dowel action ($V_{s1}$, $V_{sw1}$) and shear resistance ($V_{s2}$, $V_{sw2}$); d) sliding resistance of concrete friction ($V_{c\_\mu}$) and inclined compression stress field ($V_{c\_max}$); e) compression zone length ($x_c$) and angel of inclined compression stress field ($\alpha$)